The Temperature of the Cosmic Microwave Background Radiation at 3.8 GHz; Results of a Measurement from the South Pole Site

Giovanni De Amici [1], Marc Bensadoun [1], Marco Bersanelli [2], Al Kogut [3], Steve Levin [1][A], Michele Limon [1], George F. Smoot [1]

ABSTRACT

As part of an international collaboration to measure the low frequency spectrum of the Cosmic Microwave Background (CMB) radiation, we have measured its temperature at a frequency of 3.8 GHz (7.9 cm wavelength), during the austral spring of 1989, obtaining a brightness temperature, T_{CMB}, of 2.64±0.07 K (68% confidence level). The new result is in agreement with our previous measurements at the same frequency obtained in 1986-8 from a very different site, and has comparable error bars. Combining measurements from all years we obtain T_{CMB} = 2.64±0.06 K.

subject headings: cosmic background radiation ; Earth's atmosphere.

[1] Space Sciences Laboratory and Lawrence Berkeley Laboratory, M/S 50-232, University of California, Berkeley CA 94720, USA

[2] IFC/CNR, via Bassini 15, 20133 Milano, ITALIA

[3] Laboratory for Astronomy and Solar Physics, Code 685.3, NASA Goddard Space Flight Center, Greenbelt, MD 20771, USA

[A] present address: JPL, ms 169-506, Pasadena, CA 91109, USA

I. INTRODUCTION [a]

The low-frequency (Rayleigh-Jeans) spectrum of the Cosmic Microwave Background (CMB) is expected to contain information relevant to the physical processes that occurred in the early universe (Danese and De Zotti 1982, Burigana *et al.* 1991, and references therein). The FIRAS experiment aboard the COBE satellite (Mather *et al.* 1990) has established that the CMB spectrum above 30 GHz is a blackbody to 1% of peak brightness, leaving the low frequency Rayleigh-Jeans spectrum as the only possible place where large distortions could be detected.

Our group at Berkeley has been involved in designing and performing precise ground-based measurements of the low-frequency spectrum of the CMB since 1980; previous results from measurements by us and our collaborators at 0.6, 1.4, 2.5, 4.75, 7.5, 10, 33 and 90 GHz have greatly improved the accuracy of the spectral data in the Rayleigh-Jeans region (e.g. Kogut *et al.* 1991, Smoot *et al.* 1985, 1987, De Zotti 1986). The measurement reported here constitutes the fourth year effort with a receiver working in the 3.5-4 GHz frequency band. The results from the previous observations have been reported by De Amici *et al.* (1988, 1990), and the reader is referred to those papers for any detail not covered in this work.

II. MEASUREMENT CONCEPT AND TECHNIQUE

A microwave radiometer is a receiver whose output signal, S, is proportional to the input power, P, and is calibrated in units of antenna temperature, T_A. For a blackbody at a thermodynamic temperature T covering the aperture of the antenna:

$$T_A = \frac{P}{kB} = \frac{T_\nu}{e^{(T_\nu/T)} - 1} \qquad (1)$$

where $T_\nu = h\nu/k$ (=0.1825 K at 3.8 GHz), h is Planck's constant, ν is frequency, B is bandwidth, and k is Boltzmann's constant.

---

[a] Unless otherwise specified, all error bars given in this paper are 68% confidence level limits (1-σ level).

When the radiometer is pointed at the zenith, the received power in antenna temperature, $T_{A,zenith}$, is the sum of many contributions:

$$T_{A,zenith} = T_{A,CMB} + T_{A,galaxy} + T_{A,ground} + T_{A,atm} \quad (2)$$

where the attenuation due to the atmosphere ($\approx 0.3\%$) has been neglected in this discussion, but not in the numerical analysis, and $T_{A,CMB}$, $T_{A,galaxy}$, $T_{A,ground}$, and $T_{A,atm}$ are respectively the antenna temperatures of the CMB, the galaxy, the ground seen through the antenna sidelobes, and the atmosphere. Each measurement compares the antenna temperature of the zenith sky with that of a reference cold load. The difference in radiometer output when comparing the sky and the cold load is [b]:

$$G\,(S_{zenith} - S_{load}) = T_{A,zenith} - T_{A,load} + \Delta T_{sys} \quad (3)$$

with: $$\Delta T_{sys} = \Delta T_{inst} + \frac{\Delta G}{G}\,(T_{A,load} + T_{sys}) + \Delta R\,(T_{sys} - T_{A,load}) + \Delta L\,(T_{phys} - T_{A,load}) \quad (4)$$

where G is the calibration coefficient of the receiver, S is the output signal when viewing the zenith or the cold load, $\Delta G/G$ represents the fractional change in calibration coefficient between the upright and upside down position, ΔR is the change in reflection coefficient of the horn and amplifier, ΔL is the change in insertion loss (attenuation of the incoming signal) of the radiometer, T_{phys} is the physical temperature of the components, T_{sys} is the system temperature of the receiver, and ΔT_{inst} is the position-dependent change in receiver output. The last term in eq. (3) can be evaluated by rotating the radiometer, looking at its output with warm and cold loads, and estimating a cumulative effect for the four terms of eq. (4).

The instrument used for this experiment is a total power, direct RF-gain radiometer. The instrument is the same one used in 1987 and 1988, and described in De Amici *et al.* (1990). Because of the lower ambient temperature at the 1989 experimental site (typically -25°C) than at the site used in 1986-1988, we reduced the thermal set point of the radiometer; this in turn modified

---

[b] this formulation for eqs. 3 and 4 replaces the incorrect one given by De Amici *et al.* (1990)

the gain of the amplifiers, and the ratio between "low" and "high" gain setting. In 1989 the ratio was 2.136±0.008 and was measured many times during the data taking nights.

The experiment was carried out from a temporary camp about 1.8 km away, in the direction of 30° W longitude, from the Amundsen-Scott Research Station at the geographical South Pole, in Antarctica. The station lies on an ice field, 2800 meters above sea level, and its remoteness provides ideal conditions for avoiding man-made radio frequency interferences (RFI). The high altitude and extremely cold weather reduced the amount of atmospheric precipitable water content to less than 1.4 mm (corresponding to less than 0.05 K in antenna temperature) during our stay at the site.

Data with the cold load at liquid helium (LHe) temperature were taken during 14, 15, 16 and 17 Dec 1989 (UT). In the same period, our group operated radiometers at 90, 7.5, and 1.5 GHz; a companion group from the University of Milano operated radiometers at 0.82 and 2.5 GHz. Results from those experiments have been reported by Sironi, Bonelli & Limon (1991a,b).

III. GALACTIC MEASUREMENTS

The galactic and extragalactic radio background is modelled from existing maps of galactic emission at lower frequency (Haslam *et al.* 1982), which cover the austral region, and from a compilation of HII sources. Surveys of HII emission for the polar caps, however, are less complete than for lower latitudes. We verified the accuracy of the model (a frequency-scaled, beam-fitted extrapolation) by conducting differential measurements of the galactic emission at 30° from the zenith toward the North and South directions. We used the same technique as at the White Mountain site (see: De Amici *et al.* 1990), and corrected the data for the different atmospheric signal caused by slightly asymmetric (about 0.8°, for less than 0.014 K in atmospheric temperature) zenith angles. The results are summarized in Figure 1. A more complete discussion of these measurements, and similar measurements at 1.5 and 7.5 GHz, is in preparation. The good agreement between the frequency-scaled model and the results of the measurements, and the satisfactory closure of the data set over a 24 hour period are evident. The average difference

between the measurements and the model of scans at 30° from zenith is 0.002 K, with r.m.s. of 0.008 K.

The zero level of the data used in our model has an uncertainty of ±4 K at 408 MHz, which translates into a ±0.009 K uncertainty in the predicted galactic correction; to that uncertainty we must add those deriving from the residual scatter between our data and the model (±0.008 K), from the fact that our scans were done 30° away from the zenith (the region of direct interest for CMB measurements) and from the measured antenna beam pattern: we estimate that the galactic correction during CMB measurements is uncertain to about 0.015 K. We use ±0.008 K for differential (atmospheric emission) measurements of the sky at 30° and 40° from zenith, where the uncertainty in the zero level tends to cancel out.

IV. ATMOSPHERIC MEASUREMENTS

The atmospheric signal was measured by correlating, as a function of zenith angle, the signal received by the radiometer with the air mass observed.

Each "measurement" of the antenna temperature of the atmosphere consisted of several "scans"; one scan involves pointing the receiver, in order, toward the 40°N, 30°N, zenith, 30°S, and 40°S positions. Due to instrument and wind-fence layout, there was a lower and less-cluttered horizon in the North direction; scans would then often omit the South positions. After every scan, and at the beginning and at the end of each measurement, the radiometer was calibrated by comparing the signal from the sky with the signal from a known ambient temperature load. Statistical uncertainty in the measured atmospheric signal is twice as large for the 30° values as for the 40° ones; total uncertainty, which is dominated by systematics, scales in a similar way. The values from each angular set were averaged together and the average constitutes the result of a scan. The scans were then averaged together to give a value for a measurement.

The results of all atmospheric measurements are reported in Table 1 with the statistical error caused by random spread of the results of the scans. Figure 2 shows the distribution of the results from all scans and from all measurements. The best indicator of the average antenna temperature of

the atmosphere is the average of the measurements from different days, which (with statistical error only) is 1.109±0.004 K.

Possible errors in our measurements are caused by errors in the atmospheric and galactic models we use, subtraction of the sidelobe contribution, the size of the antenna beam, the pointing of the antenna, the correction to the data induced by saturation in the receiver, position-dependent changes in the gain or the offset, and uncertainties in the value of the receiver's calibration constant. These uncertainties cannot be reduced simply by taking more data. Table 2 summarizes the estimated contribution of each element. Systematic errors that were not significantly modified with respect to the 1988 experiment are only briefly discussed here.

The presence of the Sun above the horizon at all times adds another component to the total sky signal. For an antenna beam much larger that 0.5°, the Sun's apparent brightness temperature at 3.8 GHz ranges from 27,000 K, during minima of the sunspot cycle, to 44,000 K during maxima (Allen, 1973). December of 1989 was a period of increasing solar activity; we modelled the Sun as a blackbody at 40,000 ± 4,000 K of diameter 0.5°, and included this correction in the analysis. The low declination and good off-axis rejection by the antenna make the solar contribution negligible (less than 0.001 K) during vertical observations, small for the 30° position (0.002 K), and of some importance only for the 40° position (0.014 K). This correction is time dependent, and affects only data taken when the Sun is within 30° from the scan direction (less than 12% of the positions). No systematic difference was detected between the positions corrected for the Sun signal and those uncorrected. Because of the uncertainties in the solar correction and the relatively small number of data points affected by it, those data have been excluded from the final analysis.

We observed the frequency spectrum of the received signal a few days before and after the data-taking nights; no RFI signal was detected at the 0.002 K level.

Ground thermal emission and stray radiation pickup through the sidelobes of the antenna were reduced by the use of an antenna of high directivity and a ground shield. On the North side of the observing platform, we covered about 100 m^2 of ice with aluminum sheets, to further reduce

its emissivity. We measured a sidelobe contribution of 0.006±0.008 K when looking to the zenith; looking to the North we got 0.005±0.009 K at 30°, and 0.006±0.009 K at 40°, while to the South, (the direction toward the other radiometers, the station and where the ice is not covered by metal sheets) we got 0.010±0.010 K at 30°, and 0.015±0.012 K at 40°. These measurements are in good agreement with the results of modelling the ice (as a dielectric) as seen by diffraction over the shields, which predict 0.004 K for the vertical position, 0.007 K for 30°, and 0.010 K for 40°. The data have been corrected for the measured effect, and the uncertainties (added in quadrature) taken as the uncertainty of the correction.

The calibration coefficient G is measured from the difference in signal between two loads at widely different and well known temperatures (usually an ambient and an LN2-cooled target), after allowing for saturation effects in the amplification and detection chain. Errors in measurement of the calibration coefficient, about 0.2%, derive from uncertainties in the temperature of the target and from r.m.s.. noise in the radiometer output. There is no indication of systematic differences from night to night. The uncertainty in the correction for non-linearities in the detection chain gives a 0.8% uncertainty in the value of the calibration constant. Combining the errors in quadrature gives a 0.9% uncertainty, which, for $T_{A,atm} \approx 1.1$ K, results in an error of 0.010 K. Measurements of the calibration coefficient were done before each scan; the measurements were fitted with a linear drift over each 30-minute interval (10 measurements of the gain). The autocorrelation function of the radiometer output fails to reveal any time-dependent structure in the data.

Changes in the instrument that correlate with changes in receiver position (ΔT_{sys}) have been measured after returning to Berkeley by attaching a piece of microwave absorber at temperatures above (+50 and +30°C), equal to (+18°C) and below (-10°, -30°, and -190°C) ambient temperature to the horn and then moving the radiometer between the vertical and 40° position, while the output signal was monitored. All the resulting differences are consistent with a null effect. The extrapolation to a 4 K target temperature suggests that the output change during

atmospheric measurements is 0.008±0.010 K. If the effect was due to a change in gain, then the effect (and uncertainty) would be smaller: less than 0.003 K.

Using the results of Table 2 and adding systematic and statistical errors in quadrature, we can obtain a final value and uncertainty for the atmospheric antenna temperature:

$$T_{A,atm} = 1.109 \pm 0.060 \text{ K}$$

The average is obtained by weighting the averages of each pointing angle according to their systematic uncertainty. The error bars for the 30° and 40° pointing are quite different; any way of combining the errors would reduce the estimate of the overall uncertainty. Since the error bars are not independent from each other, we took the smallest set of errors in table 2, rather than combining them together statistically.

The atmospheric antenna temperature as a function of frequency, altitude, and water vapor content can be computed from existing models (Danese and Partridge 1989, Costales *et al.* 1986). In these models, emission and absorption at 3.8 GHz is mostly due to the continuum of the oxygen molecules, with a weak (less than 10% of the total) contribution from the wings of the water lines at, and above, 22 GHz. Using a temperature and density profile which accounts for arctic summer conditions, the model (Danese, 1988, priv. comm.) predicts antenna temperatures between 1.05 and 1.13 K, in very good agreement with our measured value. Figure 3 shows the atmospheric antenna temperature at 3.8 and 90 GHz, as measured during simultaneous (or near simultaneous) data taking runs. From the 90 GHz data, we estimate that the atmospheric water vapour content ranged between 0.8 and 1.4 mm. As expected, the measurements at lower frequency show little dependency on the amount of water vapour in the atmosphere.

V. ZENITH SKY TEMPERATURE

The cold load calibrator (CLC) used for this experiment has been described by Bensadoun *et al.* (1991). It consists of a microwave absorber (emissivity ≈ 0.9999 at 4 GHz) covering the bottom of a large (78 cm wide, 130 cm deep) cryostat, which is partially filled with liquid helium, so that the absorber is completely submerged. The radiometric temperature is, to within 1%

uncertainty, the temperature of the cryogenic liquid in the cryostat. We measured the thermodynamic temperature of the boiling LHe by measuring the ambient pressure inside the CLC, and converting it to temperature via standard tables (Duriex and Rusby 1983). With an ambient pressure of 520±2 mm Hg, the radiometric temperature of the CLC was 3.762±0.019 K (see table 3 for details).

The results of the measurements of the zenith sky temperature are summarized in Table 4, and their distribution shown in figure 4. The receiver viewed three different loads during the measuring routine: the vertical sky, an ambient temperature blackbody target (used as a warm load), and the CLC. The loads were alternated according to a fixed scheme: sky, CLC (with radiometer turned upside down), sky, warm load.

After accounting for the receiver calibration constant, we obtain the signal difference between the sky and the CLC, with r.m.s. variation:

$$G\,(S_{sky}-S_{load}) = -0.009\pm0.008 \text{ K}$$

The quantity ΔT_{sys} has been measured by the same technique used for atmospheric scans, but rotating the radiometer upside down. The results were then linearly extrapolated (in temperature) to a 4 K target; the signal change is predicted to be 0.034±0.028 K. The larger error bar for ΔT_{sys} in this test is caused by the failure of a workable target at 77 K. The change could be due to changes in the target, or in the calibration constant: we adopt for our measurement of the collective effect of the four terms of eq. 4 the value of 0.034±0.034 K.

VI. TEMPERATURE OF THE CMB; RESULT AND DISCUSSION

Combining eq. (2) and (3) gives:

$$T_{A,CMB} = G\,(S_{zenith} - S_{load}) + T_{A,load} - \Delta T_{sys} - T_{A,galaxy} - T_{A,ground} - T_{A,atm} \quad (4)$$

We now have all the elements to compute the temperature of the CMB. From eq. (4) and Table 5, we can write: $T_{A,CMB} = 2.55 \pm 0.07$ K or, converting to thermodynamic temperature:

$$T_{CMB} = 2.64 \pm 0.07 \text{ K}$$

This result is in agreement with the results at this same frequency from 1986, 1987 and 1988: 2.59±0.13 K, 2.56±0.09 K and 2.71±0.07 K respectively (De Amici *et al.*, 1988, 1990). Any combination of the results from different years must take into account the fact that the errors are only partially independent. By weighting the results from each year according to its statistically independent uncertainties, and adding the independent uncertainties (in quadrature) to the correlated errors, we obtain a final result:

$$T_{CMB} = 2.64 \pm 0.06 \text{ K}$$

It is encouraging that the same value for T_{CMB} is obtained from locations where the systematic errors are expected to be as different as the White Mountain Research Station in Eastern California and the South Pole, and using two CLC as different as the ones used in 1986-7 and 1988-9; this result is also in very good agreement with other low frequency measurements obtained by us and by our collaborators (for a review, please see Kogut *et al.*, 1991 and Sironi *et al.*, 1991c), and only marginally disagrees with the high frequency measurements of the FIRAS (Mather *et al.*, 1990).

The aim of our experiment is to measure the Rayleigh-Jeans spectrum of the CMB, and the result reported here is only part of the overall effort. A complete discussion of its meaning cannot be made without reference to the results at the other frequencies; a forthcoming paper (Sironi *et al.*, 1991c) will report on that. Within the limits of a single frequency measurement, this result sets a very tight constraint on the shape of the spectrum of the CMB below 10 GHz, confirming the measurements at 2.5 GHz (Sironi and Bonelli 1986) and 4.75 GHz (Mandolesi *et al.*, 1986).

VII. ACKNOWLEDGMENTS

This research was funded in part by the National Science Foundation Grant No. DPP 8716548 and by the Director, Office of Energy Research, Office of High Energy and Nuclear Physics, Division of High Energy Physics of the U.S. Department of Energy under Contract DE-AC03-76SF00098. We wish to thank the staff of ITT Antarctic Services and of the NSF Division of Polar Program, and the crew of the Amundsen-Scott South Pole Station. We are indebted to Francesco Cavaliere,

John Gibson and Faye Mitschang for their help during different phases of this project. Additional help was provided by Harriet Aguiar, Charles Backus and Christine Ing.

M. Bersanelli acknowledges support from ENEA, Progetto Antartide; M. Limon acknowledges support from Fondazione Angelo Della Riccia.

References

Allen, C. W., 1973, *Astrophysical Quantities, 3rd edition*, (The Athlone Press, London, GB)

Bensadoun M., Witebsky, C., Smoot, G., De Amici, G. Kogut, A., & Levin, S. 1991, *Rev. Sci. Inst.*, submitted

Burigana, C., Danese, L. & De Zotti, G., 1991, *Astron. Astroph.*, in press

Costales, J., Smoot, G., Witebsky, C., De Amici, G., & Friedman, S.D. 1986, *Radio Science*, **21**, 47.

Danese, L. & De Zotti, G., 1982, *Astron. Astroph.*, **107**, 39

Danese, L. & Partridge, R.B., 1989, *Ap. J.*, **342**, 604

De Amici, G., Bensadoun, M., Bersanelli, M., Kogut, A., Levin, S.M., Smoot, G.F., & Witebsky, C. 1990, *Ap. J.*, **359**, 219.

De Amici, G., Smoot, G.F., Aymon, J., Bersanelli, M., Kogut, A., Levin, S.M., & Witebsky, C. 1988, *Ap. J.*, **329**, 556.

De Zotti, G., 1986, in A. Faessler (edt.) Progress in Particle and Nuclear Physics, **17**, 117 (Oxford: Pergamon Press)

Duriex, M. & Rusby, R.L., 1983, *Metrologia*, **19**, 67

Haslam, C.G.T., Salter, C.J., Stoffel, H., & Wilson, W.E., 1982, *Astr. Astroph. Suppl. Ser.*, **47**, 1.

Kogut, A., *et al.*, 1991, in: Holt, S., Bennet, C., & Trimble, V. (edts.); Proceedings 'After the First Three Minutes' workshop, College Park, MD (AIP, in press)

Mandolesi, N., Calzolari, P., Cortiglioni, S., Morigi, G., Danese, L, & De Zotti, G. 1986, *Ap.J.*, **310**, 561

Mather, J., *et al.*, 1990, *Ap.J. Lett.*, **354**, L37

Sironi, G. & Bonelli, G., 1986, *Ap.J.*, **311**, 418.

Sironi, G., Bonelli, G., & Limon, M. 1991a, in: Proceedings 'Texas-ESO-CERN Symposium', Brighton, UK, in press

Sironi, G., Bonelli, G., & Limon, M. 1991b, *Ap.J.* , submitted

Sironi, G., *et al.*, 1991c, *Ap.J. Lett.*, in preparation

Smoot, G., *et al.*, 1985, *Ap.J. Lett.*, **291**, L23

Smoot, G., Bensadoun, M., Bersanelli, M., De Amici, G., Kogut, A., Levin, S.M., & Witebsky, C., 1987, *Ap.J. Lett.*, **317**, 45

Table 1 - Results of atmospheric measurements done during December 1989 (only statistical error is quoted).

day	time [UT]		scan	signal and error [K]				
	from:	to:		40S [a]	30S [a]	30N [a]	40N [a]	weighted average [b]
2	10:14	11:29	35	-	-	1.084 (0.107)	1.091 (0.093)	1.089±0.013
6	13:29	15:55	31	-	-	1.094 (0.119)	1.126 (0.092)	1.123±0.015
6	18:23	19:09	21	-	-	1.123 (0.107)	1.133 (0.084)	1.128±0.019
7	05:05	05:49	17	1.105 (0.067)	1.129 (0.062)	1.116 (0.085)	1.106 (0.044)	1.110±0.010
7[c]	10:55	12:49	36	1.060 (0.092)	1.088 (0.104)	1.088 (0.141)	1.127 (0.084)	1.104±0.013
8[d]	02:30	05:04	59	1.120 (0.105)	1.082 (0.123)	-	-	1.111±0.014
9	05:12	06:12	21	1.057 (0.094)	1.120 (0.105)	1.112 (0.121)	1.081 (0.064)	1.086±0.011
11	06:03	09:52	77	1.106 (0.059)	1.141 (0.126)	1.099 (0.114)	1.105 (0.050)	1.106±0.005
14	10:46	11:25	13	1.130 (0.042)	1.120 (0.082)	1.143 (0.078)	1.121 (0.089)	1.127±0.014
14[c]	13:30	14:02	11	-	-	1.138 (0.116)	1.144 (0.029)	1.142±0.008
14[c]	15:24	16:31	21	-	-	1.097 (0.130)	1.110 (0.062)	1.108±0.013
15	12:16	12:59	15	-	-	1.105 (0.059)	1.095 (0.020)	1.098±0.007
15	14:30	15:10	25	-	-	1.105 (0.069)	1.097 (0.070)	1.098±0.012
16	07:04	07:48	26	-	-	1.105 (0.069)	1.097 (0.070)	1.123±0.013
16	08:55	09:41	26	-	-	1.120 (0.107)	1.123 (0.058)	1.122±0.010
17	06:45	07:48	33	-	-	1.130 (0.091)	1.107 (0.066)	1.109±0.010
17	09:00	09:43	25	-	-	1.160 (0.058)	1.113 (0.043)	1.123±0.008
		average [b,e]		1.103±0.006	1.101±0.008	1.109±0.006	1.112±0.004	
		data points [e]		200	203	392	394	
weighted average of the 17 measurements:[b]								1.109 ± 0.004

[a] r.m.s. uncertainty is given in parenthesis

[b] 1-σ statistical error is given

[c] the positions toward South are affected by the Sun within 30° from the beam axis, and have been disregarded

[d] the positions toward North are affected by the Sun within 30° from the beam axis, and have been disregarded

[e] some positions have been excluded from the averages because of poor data quality or operator's mistakes

Table 2 - Contributions to overall uncertainty for atmospheric antenna temperature evaluation

quantity	amount$_{A,atm}$	kind of error	uncertainty [K] at 30°	uncertainty [K] at 40°
spread of data	±0.004 K	statistical	0.004	0.004
atmospheric scale height	7±2 km	systematic	0.001	0.001
atmosph. kinetic temperature	240±20 K	systematic	0.001	0.001
diffracted earth radiation	(see text)	systematic	0.072	0.036
pointing error	± 5 '	systematic	0.007	0.005
error on value of gain	0.9% * $T_{A,atm}$	systematic	0.009	0.009
error due to gain drift	0.006 K	systematic	0.036	0.018
gain ratio uncertainty	0.4% * $T_{A,atm}$	systematic	0.004	0.004
saturation	0.001 K	systematic	0.006	0.003
beam pattern	±3° HPBW	systematic	0.020	0.020
galactic correction	0.008	systematic	0.048	0.024
radiometer offset change	±0.010 K	systematic	0.060	0.030
RFI	±0.002 K	systematic	0.012	0.006
solar emission	±0.008 K (a)	systematic	0.048 (a)	0.024 (a)
total uncertainty			0.114	0.060

(a) because of the relatively small number of data point affected by the solar correction, and the relatively large uncertainty associated with it, all those data points have been disregarded; these values are reported here for reference only, and do not enter in the computation of the final overall uncertainties.

Table 3 - Radiometric temperature of the cold load; ambient pressure was 520 mm Hg

quantity	contribution to antenna temperature [K]	uncertainty [K]
emission of cryogenically cooled target	3.752	0.002
emission of windows and gas	0.002	0.001
emission loss of walls	0.002	0.002
incoherent reflection	0.006	0.005
coherent reflection	0.000	0.018
total	3.762	0.019

Table 4 - Measured difference between vertical sky and cold load calibrator antenna temperatures. Final value is the average of all data points, with r.m.s. uncertainty.

day and time (UT)		number of data points	difference [K] average	r.m.s.
14 Dec 1989	12:01-13:15	21	-0.012	0.008
14 Dec 1989	14:16-15:05	10	0.001	0.006
15 Dec 1989	14:16-15:05	10	-0.015	0.004
16 Dec 1989	08:17-08:42	7	-0.010	0.004
17 Dec 1989	08:08-08:42	9	-0.002	0.005
average			-0.009	0.008

Table 5 - Data for measurements of antenna temperature of CMB.

quantity	amount [K]	error [K]
atmospheric temperature	1.109	±0.060
sidelobes	0.006	±0.008
position dependent output change	0.034	±0.034
cold load temperature	3.762	±0.019
galactic emission	0.055	±0.015
difference between sky and cold load	-0.009	±0.008
$T_{A,CMB}$ (according to eq. 4)	2.549	±0.074 (a) ±0.144 (b)

(a) errors have been added in quadrature
(b) errors have been added linearly

Figure captions

1 - Results of differential galactic drift scans at -60° declination, and prediction of a similar scan obtained from extrapolation of the map at 408 MHz (Haslam *et al.* 1982) and of a compilation of sources at 2.5 GHz, and fitted to the measured antenna beam pattern. The profile shown has been computed using a spectral index of 2.75 for synchrotron radiation, and of 2.1 for HII radiation. Experimental data (*filled circles*) are differences between positions 180° apart around the parallel circle; they have been corrected for ground contribution and atmospheric emission, and binned in 12-minute intervals (≈6 data points/bin). Statistical error bars are shown. The chi-square/d.o.f. is 1.3°.

2 - Histogram of the results of the antenna temperature of the atmosphere from all positions;

a) from 492 scans: average is 1.109 K, with statistical (1-σ) error of 0.004 K

b) from 1188 positions: average is 1.106 K, with statistical (1-σ) error of 0.003 K

3 - Results of simultaneous (within 3 hours) measurements of the atmospheric antenna temperature at 3.8 and 90 GHz. Error bars are r.m.s. of each measurement; typical number of scans for a 90 GHz measurement is 12, for a 3.8 GHz measurement is 30 (see also table 1). The dashed line shows the correlation slope predicted by the model.

4 - Histogram of all measurements of the temperature difference between the zenith sky and the cold load calibrator.

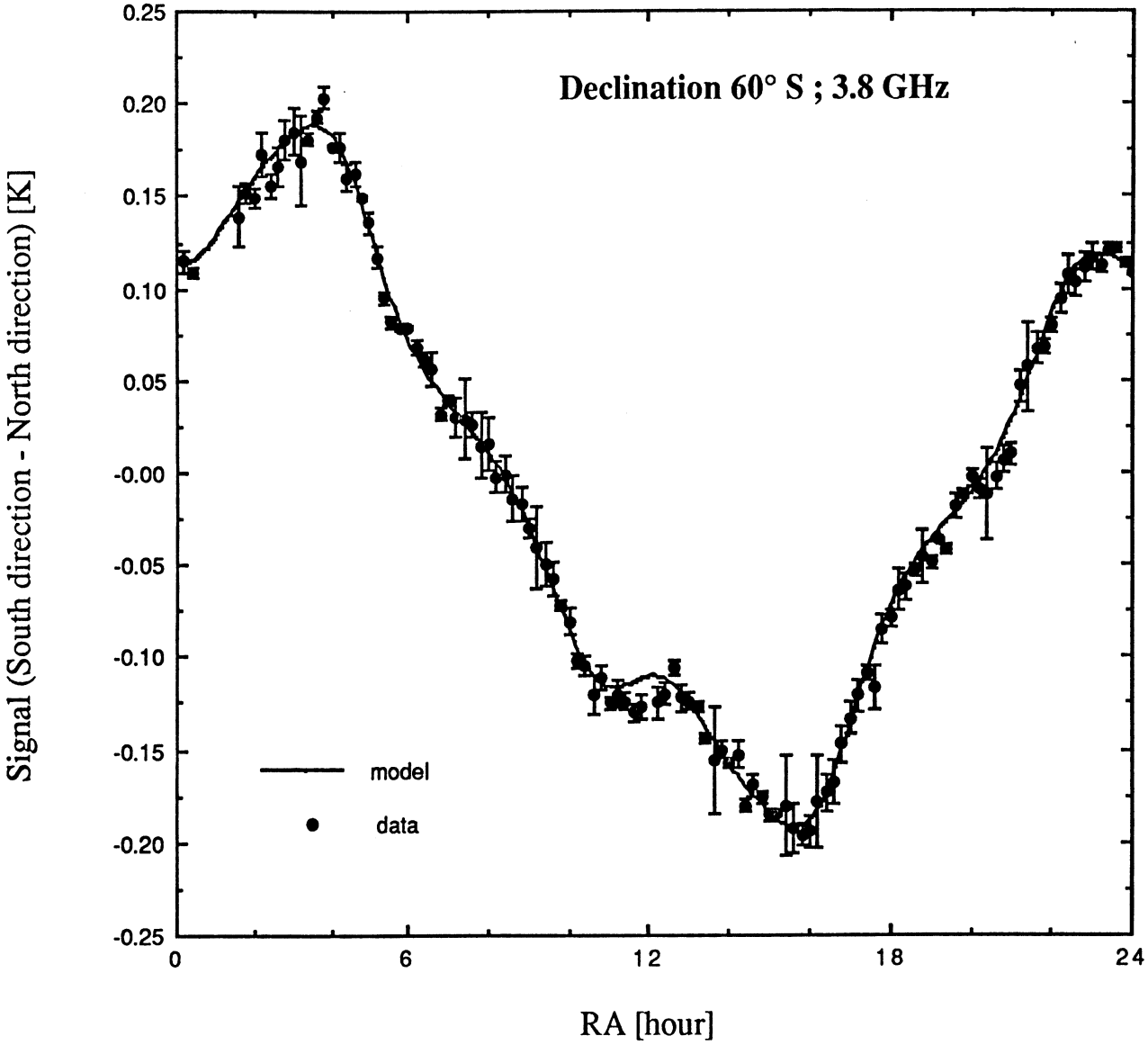
Declination 60° S ; 3.8 GHz
Signal (South direction - North direction) [K]
RA [hour]
model
data
0.25
0.20
0.15
0.10
0.05
-0.00
-0.05
-0.10
-0.15
-0.20
-0.25
0
6
12
18
24

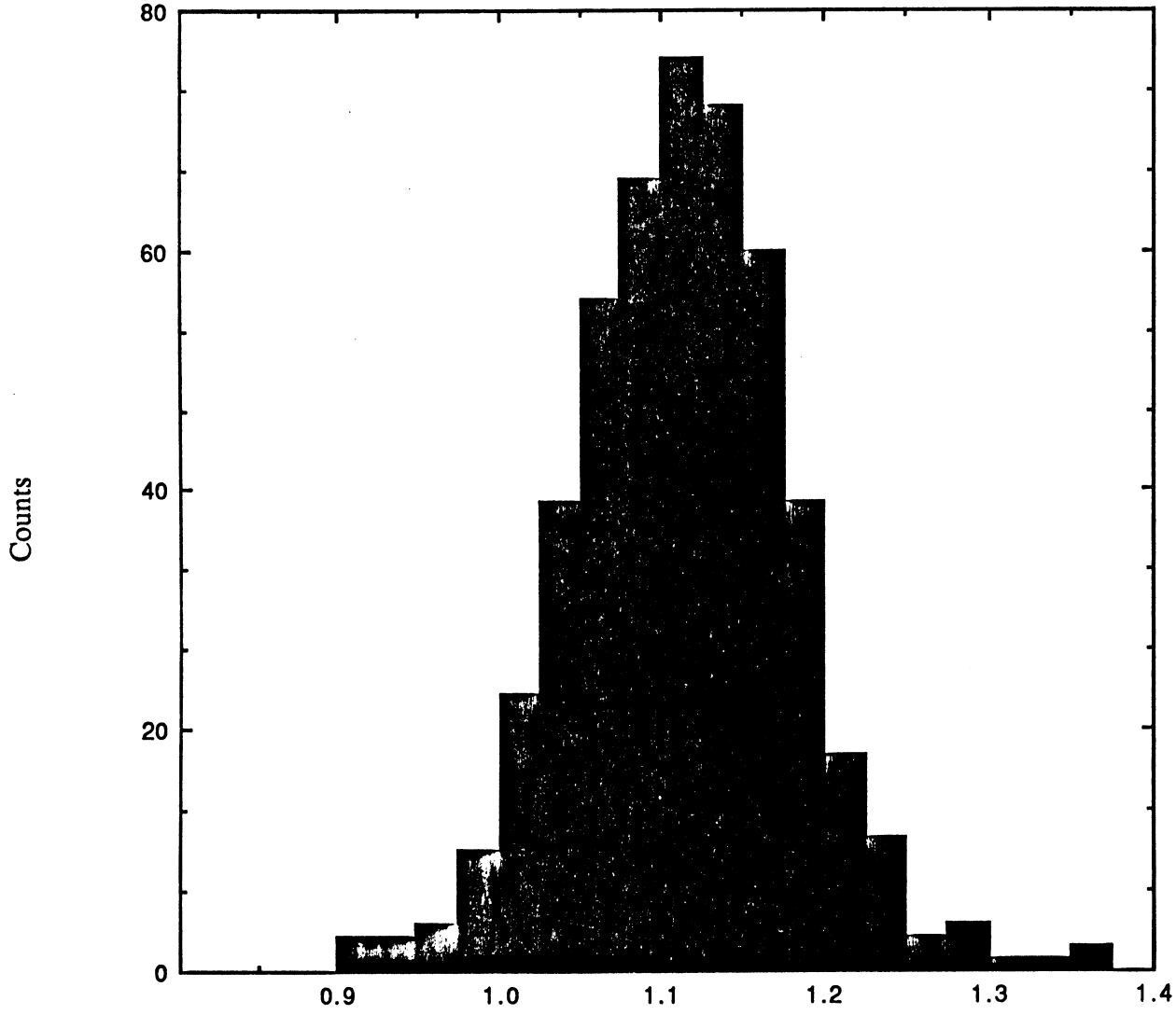
80
60
40
20
0
Counts
0.9
1.0
1.1
1.2
1.3
1.4
Atmospheric antenna temperature [K]

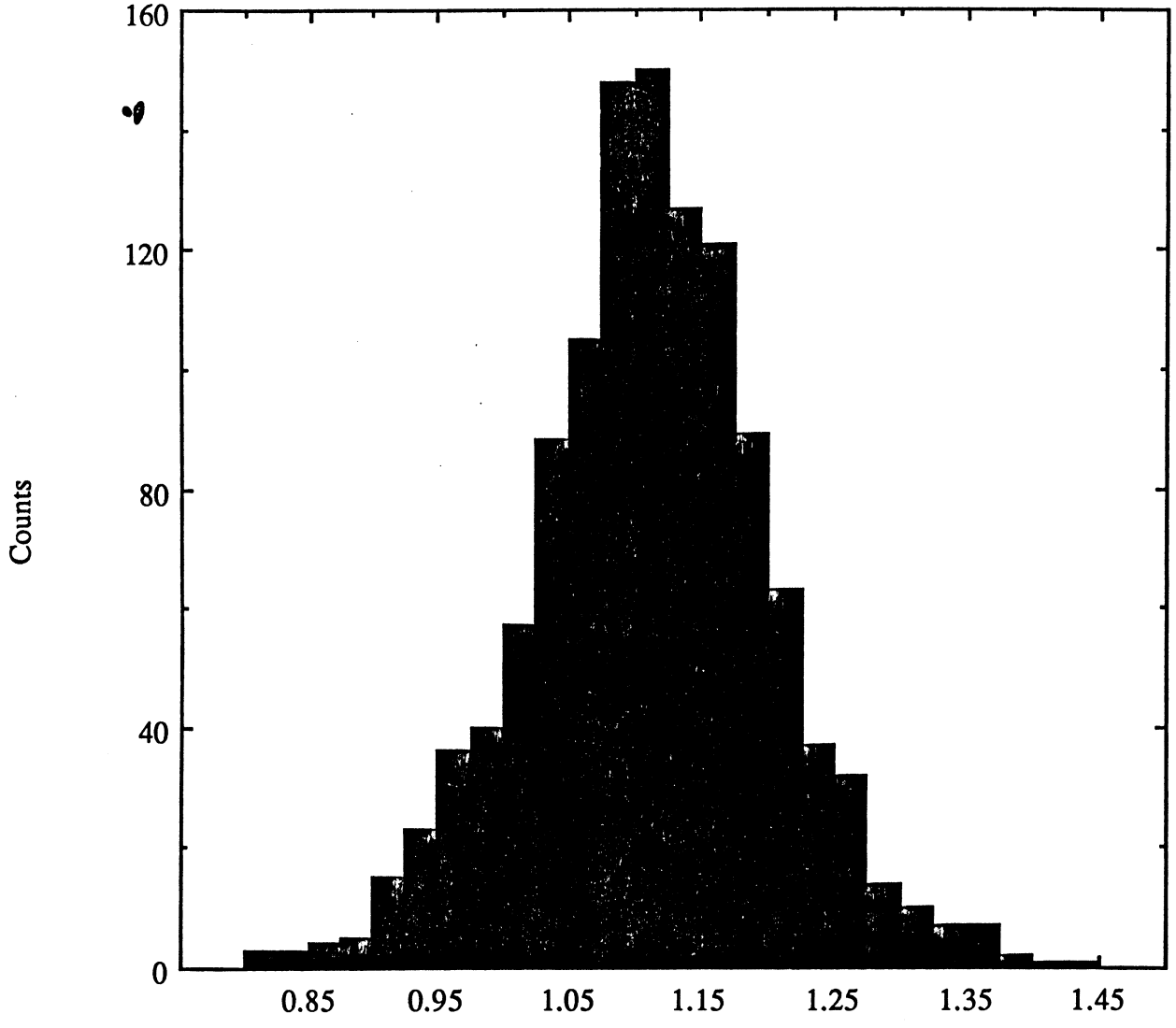
160
120
80
40
0
Counts
0.85
0.95
1.05
1.15
1.25
1.35
1.45
Atmospheric antenna temperature [K]

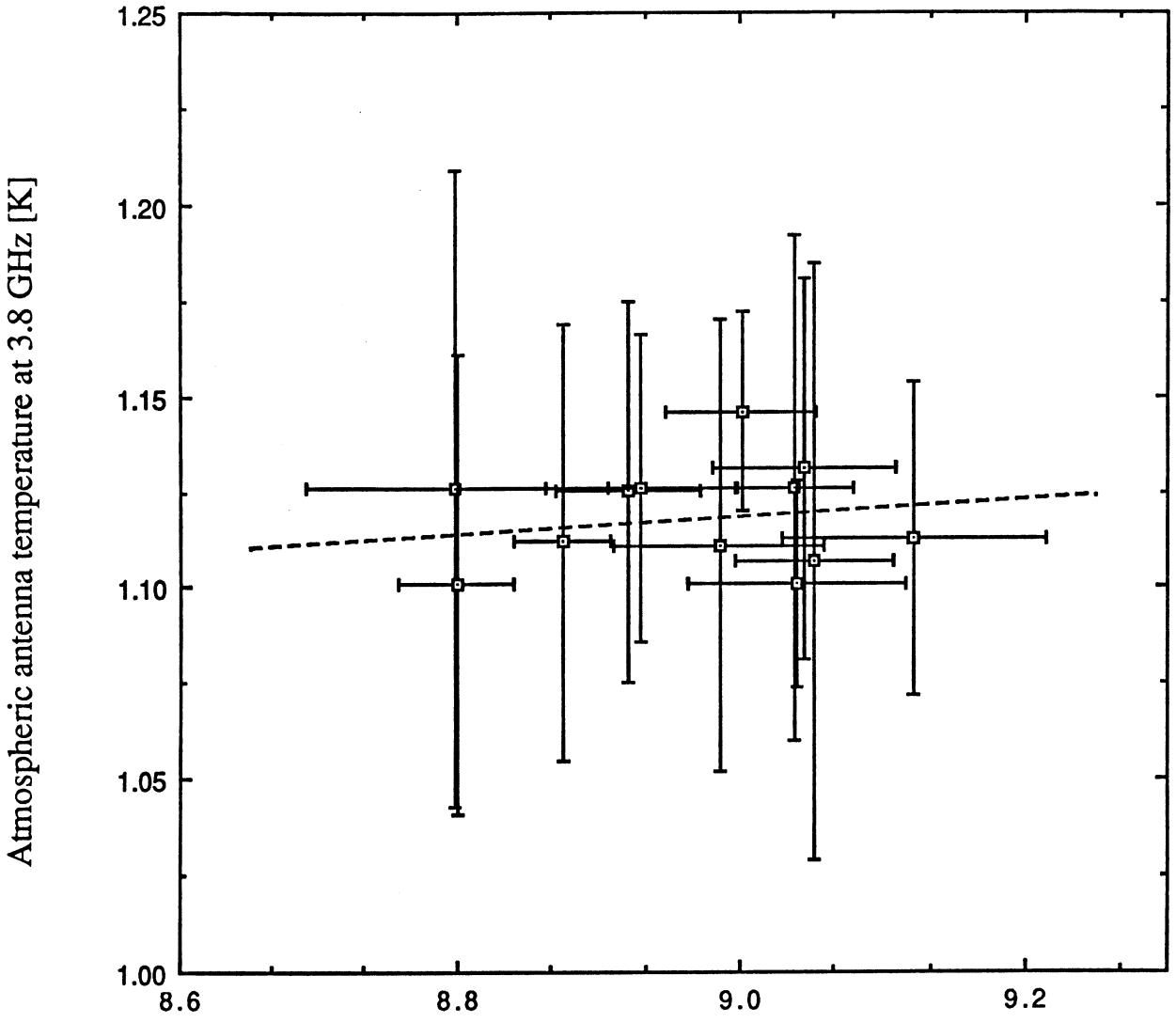
Atmospheric antenna temperature at 3.8 GHz [K]
1.25
1.20
1.15
1.10
1.05
1.00
8.6
8.8
9.0
9.2
Atmospheric antenna temperature at 90 GHz [K]

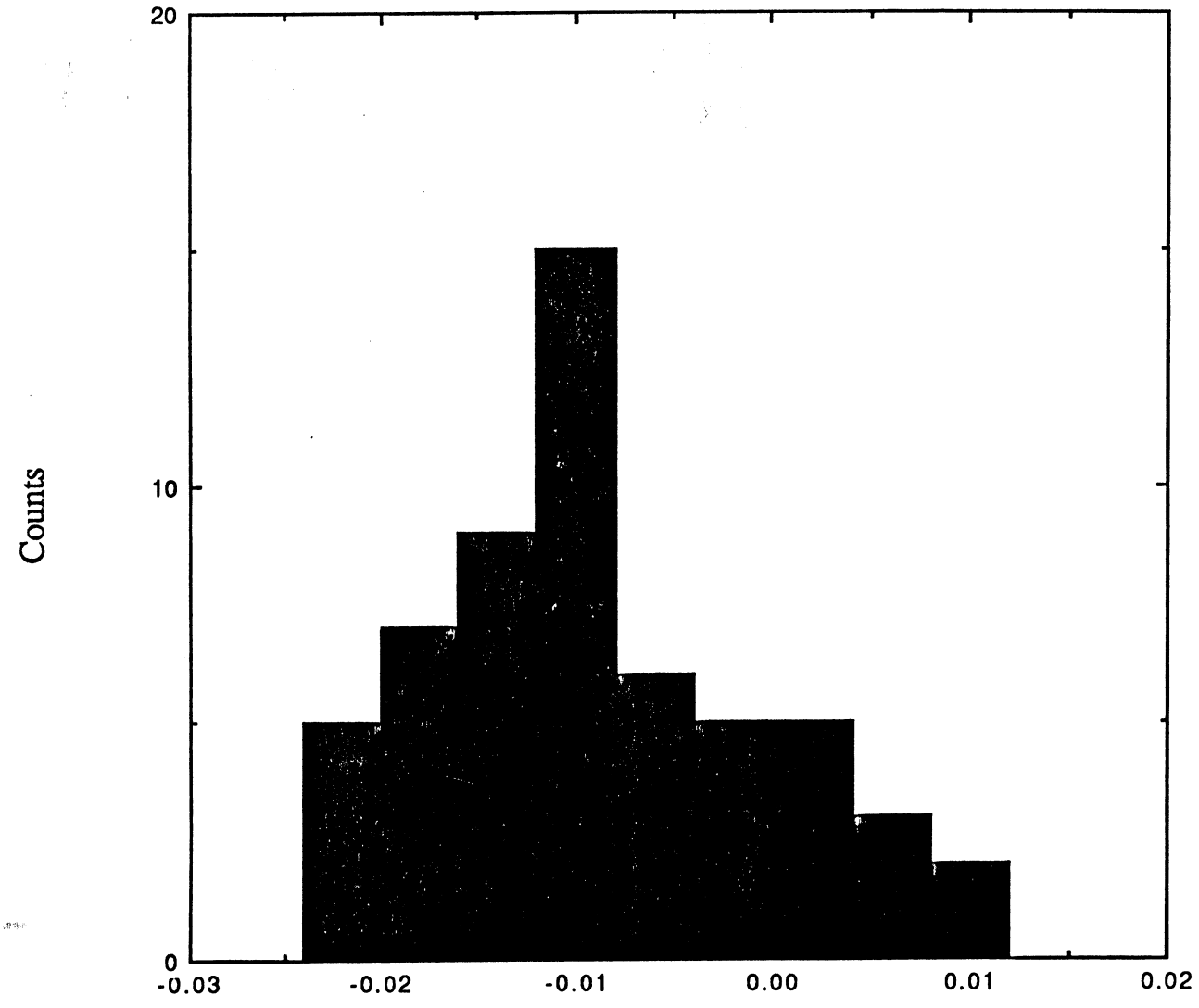
20
10
0
Counts
-0.03
-0.02
-0.01
0.00
0.01
0.02
Temperature difference between sky and CLC [K]